

Emma Longman · Katja Kreusel · Saul B. Tendler
Immo Fiebrig · Kevin King · John Adair
Paul O'Shea · Alvaro Ortega · Jose Garcia de la Torre
Stephen E. Harding

Estimating domain orientation of two human antibody IgG4 chimeras by crystallohydrodynamics

Received: 12 March 2003 / Revised: 8 April 2003 / Accepted: 8 April 2003 / Published online: 17 June 2003
© EBSA 2003

Abstract A modified crystallohydrodynamic approach introduced in 2001 is applied to two human IgG4 constructs from mouse IgG1. The constructs were point mutants of the chimeric antibody molecule cB72.3(γ 4): cB72.3(γ 4A), devoid of inter-chain disulfide bridging, and cB72.3(γ 4P), which has full inter-chain bridging. As before, the known crystallographic structures for the Fab and Fc domains were combined with the measured translational frictional ratios to obtain an estimate for the apparent time-averaged hydration of the domains and hence for that of the intact molecule. The original approach was modified with the hydrated dimensions of the domains being applied, rather than the anhydrous crystallographic dimensions, for assessing the inter-domain orientations using the algorithms HYDROSUB and SOLPRO. Both chimeric IgG4 molecules were found to have open, rather than compact, structures, in agreement with the previous study on wild-type human

IgG4. The insertion of a frictionless connector between the domains was necessary, however, for representing the cB72.3(γ 4A) chimera. It therefore appears that the inter-chain disulfide bonds act as physical constraints in the cB72.3(γ 4P) chimera, forcing the antibody domains together and producing a less elongated structure than that of cB72.3(γ 4A). The open structures produced for the two IgG4 chimeras showed similarity to those structures identified for murine IgG1 and IgG2a molecules through X-ray crystallography.

Keywords Chimeras · Crystallohydrodynamics · Disulfide bridging · Human immunoglobulin

Presented at the conference for Advances in Analytical Ultracentrifugation and Hydrodynamics, 8–11 June 2002, Grenoble, France

E. Longman (✉) · I. Fiebrig · S. E. Harding
National Centre for Macromolecular Hydrodynamics,
School of Biosciences, University of Nottingham,
Sutton Bonington, LE12 5RD, UK
E-mail: sbxejl@nottingham.ac.uk
Tel.: +44-(0) 115 951 6149

K. Kreusel · S. B. Tendler · I. Fiebrig
Pharmaceutical Sciences, University of Nottingham,
Nottingham, NG7 2GG, UK

K. King
Pfizer Limited, Sittingbourne, Kent, ME9 8AG, UK

J. Adair
Celltech Therapeutics, Bath Road, Slough,
Berkshire, SL1 4EN, UK

P. O'Shea
School of Biomedical Sciences, Queen's Medical Centre,
University of Nottingham, Nottingham, NG7 2UH, UK

A. Ortega · J. Garcia de la Torre
Departamento de Química Física, Facultad de Química,
Universidad de Murcia, 30071 Murcia, Spain

Introduction

X-ray crystallography and NMR spectroscopy are now routinely used to determine protein structure at high resolution. However, the upper limit of molecular mass in NMR studies is $\sim 50,000$ Da, thus excluding the study of the human immunoglobulin IgG4 which has a molecular mass of more than 146,000 Da. Another drawback is that electron density maps from crystallography of antibodies tend to be obscured due to flexibility in the hinge region. Although of necessarily (very) low resolution, macromolecular hydrodynamic techniques, on the other hand, are relatively quick and non-destructive and can represent the conformation of the protein in a dilute solution – the environment in which many exist naturally. They can provide overall or “gross” conformation information of the human IgG subclasses, giving the time-averaged spatial orientation of the Fab and Fc domains relative to each other (Carrasco et al. 2001). They are therefore useful for providing complementary information to that produced by the high-resolution techniques and can be used in conjunction with the high-resolution structural information available for the individual domains.

We would like to stress at the outset that although high-resolution information can be entered into hydrodynamic analysis, high-resolution information is not returned, a limitation which unfortunately is not always appreciated. Furthermore, an important drawback that limits the application of hydrodynamic methods is the influence of non-conformational parameters on the hydrodynamic properties; the most important of these is the time-averaged effect of water association with the protein or “hydration” that is very difficult to estimate with any precision. Another drawback is that the most sophisticated shape for which hydrodynamic parameters can be calculated exactly is still the ellipsoid (Harding 1989; Harding et al. 1997). Although the overall conformation of antibody domains may be represented by equivalent ellipsoids, the intact immunologically active structure cannot be represented by either axially symmetric (prolate/oblate “ellipsoids of revolution”) or centrally symmetric (“general tri-axial ellipsoid”) shapes. Good approximations are available in terms of multiple-sphere array or “bead models”, and have been thoroughly checked against ellipsoids, yielding errors, if applied correctly, of no worse than $\sim 2\%$ for parameters based on the translational frictional property. Bead modelling strategies can therefore be applied with considerable confidence for representing domain orientations of antibodies, but not for determining molecular detail.

For a typical globular protein, fine structural details (crevices, pockets, protrusions, etc.) can make a relatively large contribution to the hydrodynamics. However, for more multi-subunit structures (antibodies are a paradigmatic example) it seems evident that the main aspect is the arrangement of the subunits: whether or not there is a hinge (which may be flexible) and whether the conformation is more open or closed. As mentioned before, there is the complicating effect of hydration. Therefore, it is really justified to reduce the complexity of the problem by making structural approximations for the subunits, thus allowing us to concentrate on their spatial arrangement. This approach also greatly facilitates the modelling of the flexibility between domains, as is considered in a sister paper to this one (Garcia de la Torre et al. 2003).

Despite our detailed knowledge of the primary structure, and, in the case of IgG (and now IgE), high-resolution structures for the Fab' and Fc domains, previous attempts to find the solution conformation of intact antibodies have proven difficult (Carrasco et al. 1999, 2001). Information on how the primary amino acid sequence affects the solution structure of intact, immunologically active antibodies is therefore scarce. An early attempt to characterize the solution properties of rat IgE, based on comparing its hydrodynamic properties with a hingeless mutant IgG molecule, “IgGMcg”, whose high-resolution crystal structure was known, was the first to successfully show that IgE was cusp shaped in solution (Davis et al. 1990). More recently, Carrasco et al. (1999, 2001) introduced a new

procedure for assessing the low-resolution conformation of intact antibodies in solution in terms of the orientation of the Fc and Fab' domains relative to each other. In this procedure the shape of the individual domains from the crystal structure is combined with the experimental measurement of the translational frictional ratio from hydrodynamic measurements to yield an estimate for the time-averaged apparent hydration of the domains (δ_{app}). δ_{app} is referred to as “time-averaged” in the sense that hydration is a dynamic rather than a static process. It is referred to as an “apparent” hydration because besides volume effects it also includes the contribution of all other non-conformational and non-mass factors to the frictional coefficient. The value calculated for δ_{app} depends not only on the true hydration but is also affected by the fact that (1) the domains are not true ellipsoid structures, (2) the domains have considerable surface rugosity, and (3) small imperfections in the bead model approximation exist (the hydrodynamic parameters for a bead and bead-shell model cannot be calculated exactly, as they can for ellipsoids). The δ_{app} for intact IgG antibody molecules was thus evaluated and this value, when combined with the experimentally measured translational frictional ratio of the intact antibody molecule, provided a route to obtaining the solution conformation of the intact molecule.

In this way, Carrasco et al. (2001) were able to demonstrate that all the IgG subclasses investigated (IgG1, IgG2, IgG3 and IgG4) had open rather than compact conformations; an example of such a model is given in Fig. 1. We now seek to further apply this methodology to the study of two interesting point mutations of a chimeric antibody of the IgG4 subclass molecule cB72.3. The two IgG4 cB72.3 chimeras recognize a mucin-like tumour-associated glycoprotein, TAG-72 (Kreusel et al. 1994).

Wild-type human IgG4 is known to exist in two forms, with disulfide bonding being present between the heavy chains in the hinge regions of one form, but absent in the other. IgG1 and IgG2, however, exhibit no such heterogeneity. By looking at the hinge sequences of these human IgG subclasses, it was found that whilst a proline residue was present at position 241 of the IgG1 and IgG2 gamma chain, a serine was

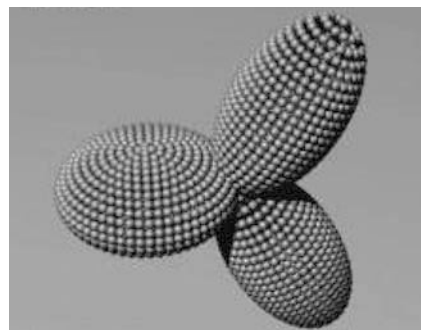


Fig. 1 Bead-shell model for human IgG4 (adapted from Carrasco et al. 2001)

present in the case of IgG4. This single amino acid variation in the hinge region was found to be the cause of the heterogeneity of disulfide bonding in human IgG4 (Angal et al. 1993).

Specifically, the two IgG4 chimeras studied were cB72.3(γ 4P) and cB72.3(γ 4A). The former was engineered so as to guarantee the hinge region was always disulfide bonded; the latter was engineered to prevent such disulfide bridge formation (Kreusel et al. 1994). Under non-reducing conditions, the non-disulfide bonded c72.3(γ 4A) chimera was present in the normal tetrameric form, with two heavy and two light chains. It was therefore evident that the two heavy chain/light chain dimers in this chimera were held together by non-covalent interactions.

With differential disulfide bonding in the hinge regions of these two chimeras, a difference would be expected in their overall structure. This study was designed to identify such structural differences, using the crystallohydrodynamics approach, based on sedimentation coefficient measurements.

Theory

Background to modelling methods

For the last two decades, bead modelling approaches have been popular for modelling the hydrodynamic properties of macromolecules, with the overall shape of the macromolecule being represented as an array of spheres of either uniform or non-uniform size (see, e.g. Garcia de la Torre 1989; Byron 1992, 2001; Carrasco 1998; Carrasco and Garcia de la Torre 1999 and references cited therein). An alternative approach is to represent only the surface of the particle with identical “minibeads”, in what is known as a bead-shell model. Such bead-shell models are not only valuable for calculating hydrodynamic parameters, but a decrease in the size of the beads enables a closer representation of the surface (Garcia de la Torre and Carrasco 2002). The hydrodynamic properties of multiple sphere arrays – beads or shells – although approximate, can be calculated to a high but finite degree of accuracy (normally better than $\sim 2\%$).

In the studies of Carrasco et al. (1999, 2001) the main parameter used for representing the solution conformation for the human IgG antibodies was the Perrin function P , or “translational frictional ratio due to shape”. The Perrin function is a universal shape parameter, meaning it is independent of the size of the particle, and therefore the shape of the particle alone determines the value. In order to obtain the Perrin function of a particle, its sedimentation coefficient must first of all be combined with the partial specific volume and molecular weight, in order to gain the translational frictional ratio (f/f_0). The translational frictional ratio is defined as “the ratio of the frictional coefficient of the

macromolecule to that of a sphere of the same mass and anhydrous volume”. In terms of experimental parameters:

$$(f/f_0) = \left(M(1 - \bar{v}\rho_0)/N_A s_{20,w}^0 \right) / \left[6\pi\eta_0(3M\bar{v}/4\pi N_A)^{1/3} \right] \quad (1)$$

in which M is the molecular weight (g/mol), \bar{v} is the partial specific volume (mL/g), N_A is Avogadro’s number and $s_{20,w}^0$ is the sedimentation coefficient (s , S) corrected to the standard conditions of density (ρ_0 , g/mL) and viscosity (η_0 , Poise) of water at 20.0 °C, and extrapolated to infinite dilution.

In order to find the Perrin function value from the translational frictional ratio, the time-averaged apparent hydration value (δ_{app} , in grams of water per gram of protein) for the particle must be known:

$$P = (f/f_0) = \left(1 + (\delta_{app}/\bar{v}\rho_0) \right)^{-1/3} \quad (2)$$

With the hydration value already available for the Fab domain (Carrasco et al. 1999), Carrasco et al. (2001) used the same approach to estimate the hydration value for the Fc domain. This approach was to fit an inertial triaxial ellipsoid to the surface of the crystal structure of the Fc domain. The two axial ratios a/b and b/c (Carrasco et al. 1999, 2001) from this ellipsoid are then entered into the routine ELLIPS2 (Harding et al. 1997), which specifies the value of P . P , and the experimental (f/f_0) for each domain, then yield δ_{app} . δ_{app} for the whole antibody is ca. $\{2\delta_{app}(\text{Fab}) + \delta_{app}(\text{Fc})\}/3$. This value, combined with the experimentally measured (f/f_0) for the intact antibody, then yields an experimental P , which can be compared with the P values calculated for the various bead models.

When piecing the molecule together, ellipsoids cannot be used directly, but have to be converted to surface bead-shell models for the hydrodynamically equivalent ellipsoids of revolution. Carrasco et al. (1999, 2001) showed that the calculated P values for the bead-shell models were in excellent agreement with those for ellipsoid models. Combining the frictional ratio of the particle with its Perrin function gives the apparent hydration value, δ_{app} (Eq. 2). The apparent hydration value for the intact antibody can therefore be found once the apparent hydration values for the Fc and Fab domains are known. Using this procedure, Carrasco et al. (2001) found IgG4 to be effectively T-shaped and hingeless, resembling the hingeless mutant antibody IgGMcg, shown to be in agreement with X-ray crystallography (Rajan et al. 1983).

The approach of antibody modelling we use in this work is similar to that used by Carrasco et al. (1999, 2001), but with a few modifications. The hydration values obtained previously for the Fc domain (Carrasco et al. 2001) and the Fab domain (Carrasco et al. 1999) were used to find the Perrin functions for both the Fc and Fab domains and the intact antibodies.

Improvements to the Carrasco approach

We follow the same approach introduced before (Carrasco et al. 2001) to estimate the apparent time-averaged hydration of an IgG antibody, i.e. from representing the crystallographic structure of the individual domains as a smooth ellipsoidal surface shell-bead model, calculating the Perrin translational frictional ratio due to shape, P , and comparing this with the experimentally obtained translational frictional ratio, f/f_0 , to give the apparent time-averaged hydration, δ_{app} , for each domain. Hence δ_{app} of the intact IgG can be estimated on the basis of IgG having two Fab and one Fc. This value is necessary to calculate the experimental P from f/f_0 for the intact antibodies, whose crystal structures are generally not known. The small improvement we make here is that when modelling the assembled domains, even though P is size-independent, we take into account the effect of different hydrations on the relative dimensions of the domains, i.e. we find the dimensions of the ellipsoids of revolution, whose hydrodynamic properties mirror those of the antibody fragments they are representing.

Finding the relative dimensions of the hydrated domains

For an ellipsoid of revolution of axial ratio $p=a/b$ ($a>b$), with a prolate ellipsoid having semi-axial dimensions (a, b, b) , and an oblate ellipsoid having the dimensions (a, a, b) , a and b can be obtained provided the axial ratio, p , and the hydrated volume of the particle (V_{hyd}) are known:

$$V_{anh} = M\bar{v}/N_A \quad (3)$$

$$V_{hyd} = (M\bar{v}/N_A)[1 + \delta/\bar{v}\rho] \quad (4)$$

For a prolate ellipsoid:

$$V_{hyd} = 4/3\pi b^3 p \quad (5)$$

For an oblate ellipsoid:

$$V_{hyd} = 4/3\pi a^3/p \quad (6)$$

We have to assume the effect of hydration does not change significantly the axial ratio, of course, but if we are using the value for p obtained from the Perrin function, and δ (approximated as δ_{app}) both according to the crystallohydrodynamic procedure above, we can obtain an estimate for a and b for both the Fab domain (represented as a prolate model) and Fc domain (represented as an oblate model).

Method for construction of bead models: HYDROSUB

Another improvement to the Carrasco et al. (2001) approach is that we can now take advantage of using the

computer program HYDROSUB (Garcia de la Torre and Carrasco 2002) for the construction of the bead models. HYDROSUB has the capacity to build models of multi-subunit macromolecules, by modelling them as structures composed of ellipsoids of revolution and cylinders. The coordinate data can then be interfaced directly into the algorithm SOLPRO for the calculation of the hydrodynamic properties and shape functions, including the Perrin P parameter, corresponding to the bead model and domain arrangement.

To build the bead-shell model, the program requires the input of four pieces of information. For each ellipsoid, HYDROSUB requires: (1) the dimensions a and b , (2) the three Cartesian coordinates that define the position of the centre, (3) the two polar angles θ and φ that define the orientation of the main axis of the ellipsoid. There is another improvement on the methodology of Carrasco et al. (2001), who used three Euler angles; we have realized (and this is implemented in HYDROSUB) that for an axisymmetric particle the orientation is just defined by the two spherico-polar angles θ and φ (Fig. 2).

We now provide an example of how the IgG model for HYDROSUB can be constructed (Fig. 2). Fc is represented as an oblate ellipsoid, and then we place its equatorial circle on the (y, z) plane, with its centre on the negative part of the z -axis, at a distance d_3 from the origin, equal to (or slightly greater than, if we wish to consider some spacing, hinge, etc.) the longest semi-axis. Thus its coordinates are $x_{c3}=0$, $y_{c3}=0$, $z_{c3}=-d_3$. With this placement, the main axis of the oblate Fc is along the x -axis and therefore its polar angles are $\theta_3=90$, $\varphi_3=0$. Now we have to situate the two Fab's (represented as prolate ellipsoid), which will be situated above the (x, y) horizontal plane. The essential choice is that of the angles. For one of the Fab ellipsoids we adopt certain values of θ_1 and φ_1 . The distance from the centre of the ellipsoid, d_1 , to the origin will be equal to or greater than the longest semi-axis of the prolate, and the coordinates of the centre are $x_{c1}=d_1*\sin\theta_1*\cos\varphi_1$, $y_{c1}=d_1*\sin\theta_1*\sin\varphi_1$ and $z_{c1}=d_1*\cos\theta_1$. For the other Fab, d_2 is the same, and in principle there will be a variability in the choices of θ_2 and φ_2 . However, we restrict ourselves to symmetric configurations, having a "Y" or "T" shaped conformation, where the essential conformation parameter is the angle β between the two arms. Then with the values of θ_1 , φ_1 , β and the condition that Fc is on the plane of the angle or bisecting the angle, the polar angles θ_2 , φ_2 can be deduced from geometric arguments. Of course, any other choice of axes, and any other initial placement of the first subunit, can be made. The details of this description would change, but the procedure would be equivalent.

The program then builds the bead-shell model by stacking rings of mini-beads, in the direction of the symmetry axis, varying the radius of the rings to form an ellipsoidal shape (or not varying this radius in the case of constructing a cylinder). Thus, the result is a structure in

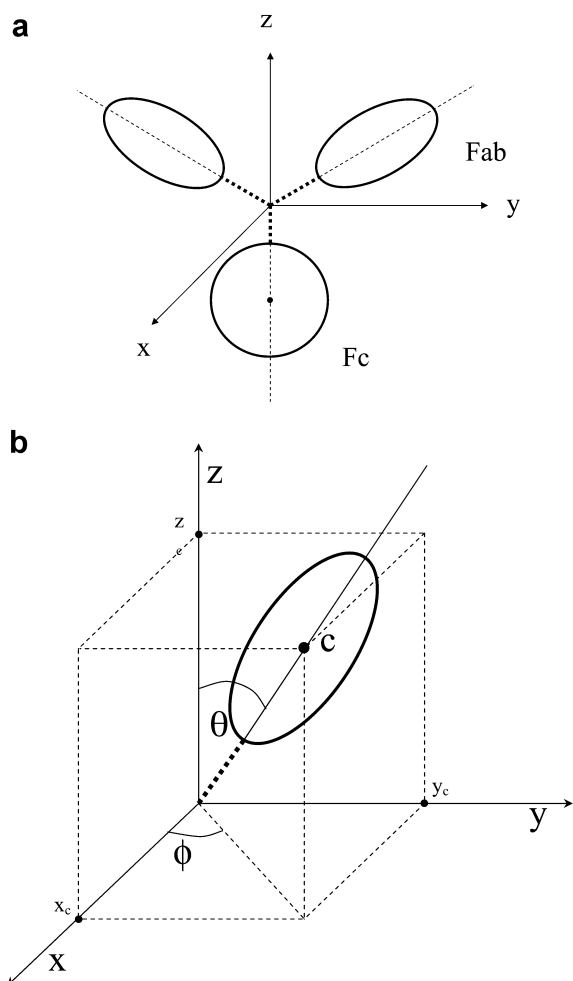


Fig. 2a, b Scheme for the construction of IgG HYDROSUB models. **a** View along the x -axis. The circle represents the oblate Fc, lying in the (y, z) plane, and the ellipses represent the prolate Fab domains, which in this example are above the (x, y) plane. The dotted lines indicate an optional separation of the tips of the subunits from the centre of coordinates (or a connector of negligible friction). **b** Definition of the Cartesian coordinates of the centre, C , of an ellipsoid, and the spherical-polar angles θ and ϕ

which the ellipsoidal surface is formed by the central points of the mini-beads.

The number of beads, N , is clearly dependent upon the number of mini-beads, and this affects the shape of the ellipsoidal surface produced and therefore the resulting properties produced by the program. In order to overcome this problem, the program calculates the value of each property, for a range of bead sizes, and then extrapolates forward to an infinite number of beads. One restriction is that the time taken to run a program to construct a shell model is proportional to N^3 , and as a result the program works with a maximum of 2000 minibeads. Once the bead-shell model of the antibody is constructed, an output file produced by HYDROSUB can be run with SOLPRO (Garcia de la Torre et al. 1997) in order to obtain the full spectrum of hydrodynamic parameters.

If the calculated Perrin function matches the experimental Perrin function of the antibody, the model represents a potential conformation for the antibody. This procedure may then be repeated many times, to investigate many different domain positions, and identify models fitting the experimental data.

Materials and methods

Materials

The samples were as previously described (Kreusel et al. 1994). The γ 4A mutant was site-specifically engineered in the hinge region to remove inter-chain disulfide bridges. The γ 4P mutant was engineered in a manner described by Angal et al. (1993). Prior to the analytical ultracentrifuge measurements, samples were extensively dialysed into filtered solutions of 50 mM $\text{Na}_2\text{HPO}_4/\text{NaH}_2\text{PO}_4$ in distilled deionized water at pH 7.

Methods

Analytical ultracentrifugation

Sedimentation coefficients, $s_{T,b}$, were obtained using an MSE Centriscan 75 analytical ultracentrifuge equipped with a monochromator and scanning UV absorption optics, set at 278 nm, at a temperature of 20.0 °C and a rotor speed of 40,000 rev/min. The scan interval was 10 min. Solution concentrations of between 0.2 and 1.0 mg/mL were used for the γ 4A mutant, and between 0.2 and 0.8 mg/mL for γ 4P.

Correction of the sedimentation coefficients measured at temperature T and in buffer b ($s_{T,b}$) to standard conditions of solvent density and viscosity (that of water at 20.0 °C) was made using the equation (Schachman 1959):

$$s_{20,w} = s_{T,b} \left\{ \frac{\eta_{T,b}/\eta_{20,w}}{\rho_{20,w}} \right\} \left\{ \frac{(1 - \bar{v}\rho_{20,w})}{(1 - \bar{v}\rho_{T,s})} \right\} \quad (7)$$

The partial specific volume was calculated using the consensus method of Perkins (1986) and was found to be 0.730 mL/g for both mutants.

The $s_{20,w}$ values were extrapolated to zero concentration using the Gralén (1944) relation:

$$s_{20,w} = s_{20,w}^{\circ} (1 - k_s c) \quad (8)$$

Using this procedure, a value of $s_{20,w}^{\circ} = 6.20 \pm 0.08$ S was obtained for γ 4A and 6.80 ± 0.10 S for γ 4P; these compare with a value of 6.73 ± 0.06 S for wild-type human IgG4 (Carrasco et al. 2001).

As a check to see if these values were affected by any problems due to chain dissociation (potentially a problem for γ 4A) or aggregation, weight-average molecular weights were obtained using the low-speed sedimentation equilibrium technique at a rotor speed of 13,000 rev/min, with data captured by UV absorption optics at 278 nm and analysed using the MSTAR procedure (Cölfen and Harding 1997), and checked against the “chemical formula” molecular weights from the amino acid sequence and carbohydrate composition data of $\sim 147,000$ g/mol. At concentrations between 0.12 and 0.50 mg/mL, both mutants appeared monomeric, although at concentrations > 0.5 mg/mL γ 4A was seen to aggregate, and at very low concentrations (< 0.1 mg/mL) γ 4A was seen to show some chain dissociation. As none of the sedimentation coefficients were measured below 0.2 mg/mL, this was not considered a problem. It is conceivable that the effects of dissociation < 0.1 mg/mL and aggregation > 0.5 mg/mL may still have had some influence in the “linear region” (0.12–0.50 mg/mL) but were self-compensating. If this were so, simple calculation based on an $s_{20,w}$ for a non-dissociated monomer of 6.20 S at 0.2 mg/mL and

Table 1 Experimental values of the Perrin function values (P_{exp}) for cB72.3(γ 4P) and cB72.3(γ 4A). Calculated from the sedimentation coefficient, $s_{20,w}^{\circ}$, molecular weight, M , partial specific volume, \bar{v} , a time-averaged apparent hydration, $\delta_{\text{app}} = 0.59 \text{ g(H}_2\text{O)/g(protein)}$, and Eqs. (1) and (2)

Antibody	$s_{20,w}^{\circ}$ (S)	M (kDa)	\bar{v} (mL/g)	f/f_0	P_{exp}
cB72.3(γ 4A)	6.20 ± 0.08	147	0.730	1.600–1.641	1.313–1.347
cB72.3(γ 4P)	6.80 ± 0.10	147	0.730	1.456–1.499	1.195–1.230

on the $s_{20,w} \approx M^{2/3}$ power law approximation for globular proteins (Smidsrød and Andresen 1979) gives $s_{20,w}$ (dissociated monomer) $\approx 3.91 \text{ S}$ and $s_{20,w}$ (dimeric aggregate) $\approx 9.84 \text{ S}$ (based). This means that in the case of dissociation only, the weight-average $s_{20,w}$ at 0.2 mg/mL would have been $\sim 6.15 \text{ S}$, whereas in the case of aggregation only it would have been $\sim 6.27 \text{ S}$. This potential error needs to be borne in mind when considering the validity of the models.

The $s_{20,w}$ values, combined with the chemical formula molecular weights and partial specific volumes, were used to evaluate the translational frictional ratios (Eq. 1), and using the value of 0.59 for the time-average apparent hydration of the IgG's (Carrasco et al. 2001), the experimental values for P could be specified. These data are summarized in Table 1.

Modelling

Using bead-shell models to find the antibody conformations

Table 2 shows the various combinations of θ and φ angles used for the construction of candidate bead shell models using HYDROSUB and their resultant Perrin function (P) values obtained from SOLPRO. The models shown in Fig. 3 were constructed with the domains being in contact with each other, without any spacing between them. Subsequent models were constructed with spaces inserted between the domains, in the direction of the projection of the main axis of the Fab ellipsoids.

Table 2 Theoretical SOLPRO Perrin function values (P) obtained for antibody bead-shell models with varying angles θ and φ . Unless otherwise stated, the position of the Fc domain is represented by the orientation angles $\theta = 90^\circ$, $\varphi = 90^\circ$. The $s_{20,w}^{\circ}$ value corresponds to a molecule of molecular mass $147,000 \text{ Da}$ and $\bar{v} = 0.730 \text{ mL/g}$. β represents the angle between the main axis of the ellipsoids representing the Fab domains. The spaces in the models represent the distances between the central point of the Fc ellipsoid and that of the Fab ellipsoid

Space	Angles ($^\circ$) between main axis of ellipsoids	$s_{20,w}^{\circ}$ (S)	P	Chimera with similar Perrin function	
None	$\beta = 90, \theta = 90, \varphi = 45/315$	7.029	1.177		
	$\beta = 80, \theta = 90, \varphi = 40/320$	7.070	1.170		
	$\beta = 120, \theta = 90, \varphi = 60/300$	7.011	1.180		
	$\beta = 120, \theta = 90, \varphi = 60/300$ (oblate, $\theta = 0, \varphi = 90$)	7.054	1.173		
	$\beta = 180, \theta = 90, \varphi = 90/270$	7.191	1.15		
	$\theta = 70, \varphi = 45/315$	7.079	1.168		
	$\theta = 70, \varphi = 40/320$	7.101	1.165		
	$\beta = 90, \theta = 45, \varphi = 90/270$	7.471	1.107		
	5 Å	$\beta = 90, \theta = 90, \varphi = 45/315$	6.85	1.208	cB72.3(γ 4P)
		$\beta = 80, \theta = 90, \varphi = 40/320$	6.891	1.200	cB72.3(γ 4P)
$\beta = 45, \theta = 45, \varphi = 57.24/122.77$		7.315	1.131		
$\theta = 45, \varphi = 90/270$		7.286	1.135		
$\beta = 90, \theta = 50, \varphi = 22.62/157.38$		7.095	1.166		
$\beta = 180, \theta = 90, \varphi = 0$		7.127	1.160		
$\beta = 90, \theta = 90, \varphi = 45/315$ (oblate, $\theta = 0, \varphi = 90$)		6.899	1.199	cB72.3(γ 4P)	
$\beta = 120, \theta = 90, \varphi = 60/300$		6.872	1.204	cB72.3(γ 4P)	
8 Å		$\beta = 90, \theta = 90, \varphi = 45/315$	7.010	1.225	cB72.3(γ 4P)
		10 Å	$\beta = 90, \theta = 90, \varphi = 45/315$	6.685	1.237
$\beta = 120, \theta = 90, \varphi = 60/300$	6.891		1.246		
10 Å	$\beta = 180, \theta = 90, \varphi = 90/270$	6.845	1.208	cB72.3(γ 4P)	
	$\beta = 90, \theta = 90, \varphi = 45/315$ (oblate, $\theta = 0, \varphi = 90$)	6.731	1.229	cB72.3(γ 4P)	
20 Å	$\beta = 90, \theta = 90, \varphi = 45/315$	6.394	1.294		
	25 Å	$\beta = 90, \theta = 90, \varphi = 45/315$	6.267	1.320	cB72.3(γ 4A)
$\beta = 120, \theta = 90, \varphi = 60/300$		6.220	1.330	cB72.3(γ 4A)	
$\beta = 180, \theta = 90, \varphi = 90/270$		6.416	1.289		

The cB72.3(γ 4P) chimera

The structures in Fig. 3, representing antibodies with no spacing between the domains, all provide P values significantly below the experimental P (P_{exp}) values determined for both of the chimeras. However, on insertion of spaces between the domains, the P value is seen to increase, as expected for more extended structures. A selection of bead-shell models with similar P values to that of the γ 4P chimera, and therefore potentially representing the structure of this chimera in solution, is shown in Fig. 4. The models matching the γ 4P chimera data contained either 5 \AA spaces between the domains and $90\text{--}120^\circ$ between Fab domains or 10 \AA between the domains and $90\text{--}180^\circ$ between Fab domains.

The cB72.3(γ 4A) chimera

Bead-shell models with Perrin functions similar to the values for the γ 4A chimera were constructed by increasing the spacing between the antibody domains. Figure 5 shows models with P values matching that for P_{exp} of the γ 4A chimera. These models have a 25 \AA space between the domains and angles of $90\text{--}120^\circ$ between the Fab domains.

Computer programs

HYDROSUB, SOLPRO and other programs for hydrodynamic modelling belonging to the HYDRO suite are of public domain. Executables for various platforms can be freely downloaded from <http://leonardo.fcu.um.es/macromol/>. ELLIPS2 and MSTAR are available from <http://www.nottingham.ac.uk/ncmh/>.

Discussion

The spacing of domains in the final, more open bead-shell model structures shows similarity to those previously produced for murine IgG1 and IgG2a molecules

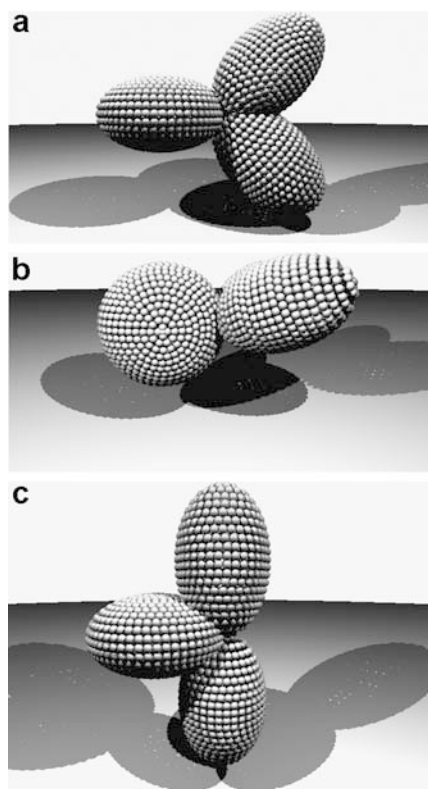


Fig. 3a–c Bead-shell models representing antibodies with no space between the domains, and variable angles θ and ϕ , and their corresponding Perrin function values

through X-ray crystallography (Harris et al. 1997, 1998). Although there may be some uncertainty with the disulfide-bond free cB72.3(γ 4A) chimera, caused by some dissociation at very low concentrations and some aggregation effects as considered above, comparison with the “intact” cB72.3(γ 4P) models suggests that removal of the disulfide bonds results in a more elongated structure. The disulfide bonds physically constrain the cB72.3(γ 4A) chimera domains, causing the domains to be brought closer together, producing a more compact structure.

Two important issues remain. Firstly, it is impossible to be more specific than comments like “more open” or “more elongated” without more experimental data from different techniques. Although, arguably, the sedimentation coefficient is the easiest and most problem-free to interpret (apart from dissociation/aggregation effects as we have seen), it is not the most sensitive to shape (see Harding and Rowe 1982; Harding 1989 for a quantitative comparison of the sensitivities of the various parameters). The intrinsic viscosity is more sensitive, but requires higher concentrations (increasing the potential problems of aggregation). Rotational diffusion-based parameters are also more sensitive, but suffer from other complications (chromophore and segmental rotation with fluorescence anisotropy measurements, and heating effects with electro-optic probes). Low- and high-angle X-ray scattering measurements have also had a notorious reputation for causing beam damage. However,

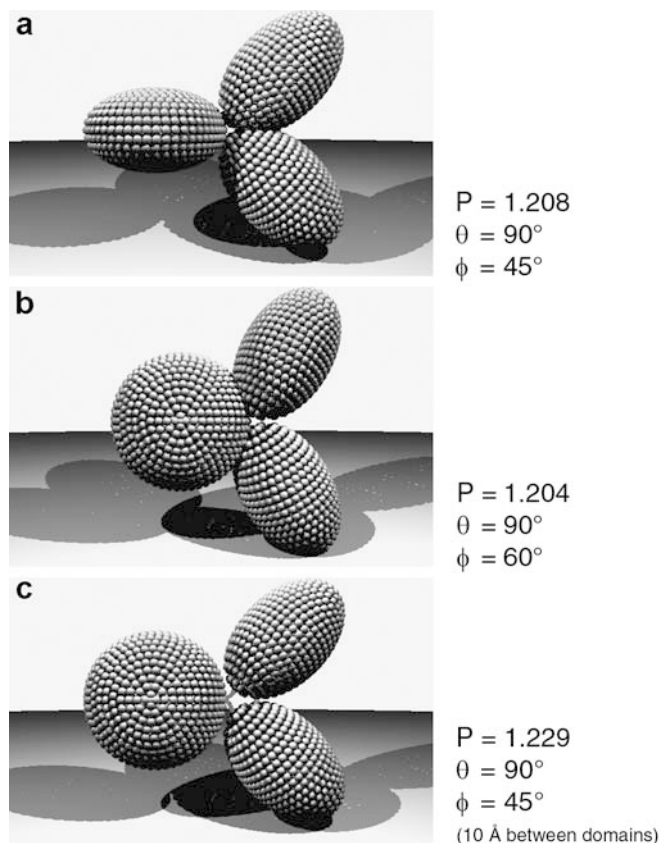


Fig. 4a–c Bead-shell models representing antibodies with Perrin function values matching that of the IgG4 chimera cB72.3(γ 4P). Part **c** shows frictionless connectors between the domains, to illustrate the approximate location of the hinge

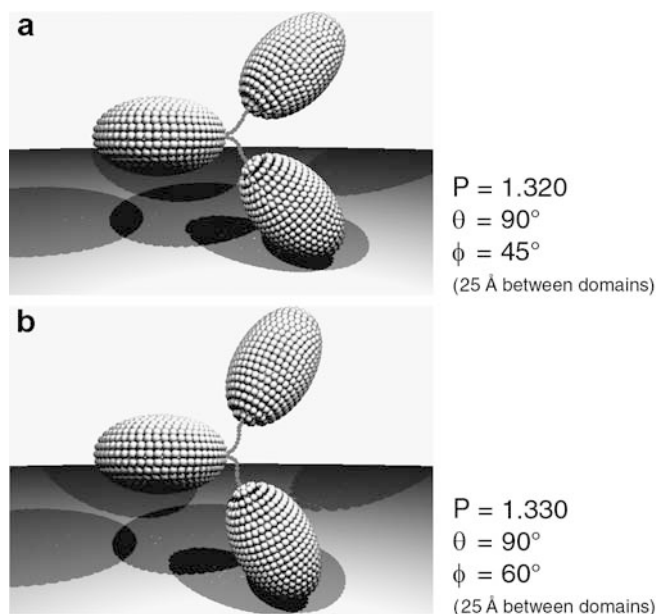


Fig. 5a, b Bead-shell models representing antibodies with Perrin function values matching that of the IgG4 chimera cB72.3(γ 4A). Both parts show frictionless connectors between the domains, to illustrate the approximate location of the hinge

steps are being made with these methods in minimizing these complications. With the extra data, and if we stick to the simple representations of domain conformations as described above, we believe the even more interesting issues such as flexibility between the domains can be rigorously addressed in the future.

It is our opinion that the representation of multi-subunit structures – to eventually include flexibility – will be one of the main challenges of 21st century hydrodynamics. For example, Garcia de la Torre et al. (2003) have considered a two-domain structure with a semi-flexible linker. In this model the subunits are also represented as ellipsoids of revolution. That study also shows that the features of the linker and the overall size and shape of the subunits are more important here than the subtle atomic details. In an earlier study, Diaz et al. (1990) tackled the problem of antibody flexibility, which may not be important in sedimentation but can be relevant in rotational/internal dynamics observed by fluorescence anisotropy decay. The approach was to use Brownian dynamics (BD) simulations of an extremely simple model, just composed of four spheres, three for the subunits and one more for the hinge.

After the “boom” of the molecular dynamics (MD) simulation with atomic resolution, both in the polymer and biophysics field, the BD approach is now considered as the most promising simulation technique for the future. Owing to the excess of detail, MD reaches quite reduced, short times, while BD can reach microseconds and further. This is thanks to the “meso-scale” structural modelling. A consequence of this meso-scale approach, which is becoming increasingly popular, is that (instead of an atomic scale), *unnecessary details are ignored in the model*, but which still retains the structural information of size, overall shape, connectivity, flexibility, etc. HYDROSUB and the tools that are being developed for flexible macromolecules belong to this class of “meso-scale” hydrodynamic modelling.

Acknowledgements This work was funded by Pfizer and Celltech Limited. Jose Garcia de la Torre acknowledges support from grant BQU2000-0229 from the Direccion General de Investigacion (Ministerio de Ciencia y Tecnología, Spain) and A. Ortega is the recipient of a predoctoral fellowship from the same agency. The comments of a referee with regards to the effects of dissociation and aggregation of cB72.3(γ 4A) are greatly appreciated.

References

- Angal S, King DJ, Bodmer MW, Turner A, Lawson ADG, Roberts G, Pedley B, Adair JR (1993) A single amino-acid substitution abolishes the heterogeneity of chimeric mouse/human (IgG4) antibody. *Mol Immunol* 30:105–108
- Byron O (1992) Solution studies on the conformation and assembly of the monoclonal antibody B72.3. PhD dissertation, University of Nottingham, UK
- Byron O (2001) Hydrodynamic bead modelling. *Methods Enzymol C* 321:278–304
- Carrasco B (1998) Propiedades de macromoleculas rigidas en disolucion: modelos, metodos computacionales y analisis de los datos experimentales. Tesis doctoral, Universidad de Murcia, Spain
- Carrasco B, Garcia de la Torre J (1999) Hydrodynamic properties of rigid particles: comparison of different modeling and computational procedures. *Biophys J* 75:3044–3057
- Carrasco B, Garcia de la Torre J, Byron O, King D, Walters C, Jones S, Harding SE (1999) Novel size-independent modeling of the dilute solution conformation of the immunoglobulin IgG Fab' domain using SOLPRO and ELLIPS. *Biophys J* 77:2902–2910
- Carrasco B, Garcia de la Torre J, Davis KG, Jones S, Athwal D, Walters C, Burton DR, Harding SE (2001) Crystalhydrodynamics for solving the hydration problem for multi-domain proteins: open physiological conformations for human IgG. *Biophys Chem* 93:181–196
- Cölfen H, Harding SE (1997) MSTARA and MSTARI: interactive PC algorithms for simple, model independent evaluation of sedimentation equilibrium data. *Eur Biophys J* 25:333–346
- Davis KG, Glennie M, Harding SE, Burton DR (1990) A model for the solution conformation of rat IgE. *Biochem Soc Trans* 18:935–936
- Diaz FG, Iniesta A, Garcia de la Torre J (1990) Hydrodynamic study of flexibility in immunoglobulin IgG1 using Brownian dynamics and the Monte-Carlo simulations of a simple model. *Biopolymers* 30:547–554
- Garcia de la Torre J (1989) Hydrodynamic properties of macromolecular assemblies. In: Harding SE, Rowe AJ (eds) *Dynamic properties of biomolecular assemblies*. Royal Society of Chemistry, Cambridge, pp 3–31
- Garcia de la Torre J, Carrasco B (2002) Hydrodynamic properties of rigid macromolecules composed of ellipsoidal and cylindrical subunits. *Biopolymers* 63:163–167
- Garcia de la Torre J, Carrasco B, Harding SE (1997) SOLPRO: theory and computer program for the prediction of SOLUTION PROPERTIES of rigid macromolecules and bioparticles. *Eur Biophys J* 25:361–372
- Garcia de la Torre J, Perez Sanchez HE, Ortega A, Hernandez JG, Fernandes MX, Diaz FG, Lopez Martinez MC (2003) Calculation of solution properties of flexible macromolecules. *Eur Biophys J* (in press)
- Gralén N (1944) Sedimentation and diffusion measurements on cellulose and cellulose derivatives. PhD dissertation, University of Uppsala, Sweden
- Harding SE (1989) Modelling the gross conformation of assemblies using hydrodynamics. The whole body approach. In: Harding SE, Rowe AJ (eds) *Dynamic properties of biomolecular assemblies*. Royal Society of Chemistry, Cambridge, pp 32–56
- Harding SE, Rowe AJ (1982) Modelling biological macromolecules in solution. 1. The ellipsoid of revolution. *Int J Biol Macromol* 4:160–164
- Harding SE, Horton JC, Cölfen H (1997) The ELLIPS suite of macromolecular conformation algorithms. *Eur Biophys J* 25:347–359
- Harris LJ, Larson SB, Hasel KW, McPherson A (1997) Refined structure of an intact IgG2a monoclonal antibody. *Biochemistry* 36:1581–1597
- Harris LJ, Skaletsky E, McPherson A (1998) Crystallographic structure of an intact IgG1 monoclonal antibody. *J Mol Biol* 275:861–872
- Kreusel KM, Adair JR, Eeley NRA, Davies MC, Jackson DE, Roberts CJ, Tendler SJB, Williams PM (1994) Conformational differences in 2 mutant hinge IgG4 antibodies observed by scanning-tunneling-microscopy. *J Vac Sci Technol B* 12:1517–1520
- Perkins SJ (1986) Protein volumes and hydration effects: the calculations of partial specific volumes, neutron-scattering matchpoints and 280-nm absorption-coefficients for proteins and glycoproteins from amino-acid-sequences. *Eur J Biochem* 157:169–180
- Rajan SS, Ely KR, Abola EE, Wood MK, Colman PM, Athay RJ, Edmundson AB (1983) 3-Dimensional structure of the Mcg IgG1 immunoglobulin. *Mol Immunol* 20:787–799
- Schachman HK (1959) *Ultracentrifugation in biochemistry*. Academic Press, New York
- Smidsrød O, Andresen L (1979) *Biopolymerkjemi*. Tapir Press, Trondheim